Journal of Agriculture and Food Research 16 (2024) 101170

Contents lists available at ScienceDirect

Journal of Agriculture and Food Research

journal homepage: www.sciencedirect.com/journal/journal-of-agriculture-and-food-research

Microwave assisted extraction of cellulose from lemon grass: Effect on techno-functional and microstructural properties

Adity Bahndral [a], Rafeeya Shams [a,**], Kshirod Kumar Dash [b,*], N. Afzal Ali [c], Ayaz Mukarram Shaikh [d], Béla Kovács [d]

[a] Department of Food Technology and Nutrition, Lovely Professional University, Phagwara, Punjab, India
[b] Department of Food Processing Technology, Ghani Khan Choudhury Institute of Engineering and Technology, Malda, West Bengal, India
[c] School of Agro and Rural Technology, Indian Institute of Technology Guwahati, India
[d] Faculty of Agriculture, Food Science and Environmental Management Institute of Food Science, University of Debrecen, Debrecen, 4032, Hungary

ARTICLE INFO

Keywords:
Cellulose
Lemon grass straw
Extraction procedure
Microwave-assisted extraction

ABSTRACT

The study focused on utilizing lemon grass straw to generate cellulose through the process of delignification, which involves the removal of hemicelluloses, followed by bleaching. The study involves the microwave-assisted alkali extraction, followed by characterizing the extracted material. At microwave power of 540 W using 8 % NaOH for 3 min for lignin removal and 540 W for 2 min for bleaching showed the maximum yield of 37.46 %. Fourier transform infrared spectroscopy is employed to analyze the physical properties of extracted cellulose, namely the hydroxyl (OH), carbonyl (C=O), C–H bonds, C–O and C–C bonds, and glycosidic linkage (C–O–C) within the cellulose polymer chain. The extracted cellulose exhibited excellent thermal stability, as indicated by its high breakdown temperature. The X-ray diffraction (XRD) analysis revealed prominent peaks at 14.8°, 16.5°, and 22.5°, demonstrating the presence of crystalline cellulose. The crystallinity index value of 70.02 % further confirmed the crystalline nature of the extracted cellulose.

1. Introduction

Agri-wastes are resulting from the cultivation and harvesting of plants and crops. Utilizing agricultural waste has the potential to effectively address the increasing energy needs of society in a sustainable fashion [1]. Cellulose, a linear homopolymer, is manufactured at a rate of 105–1010 tons each year, making it one of the most prevalent, environmentally friendly, renewable, cost-effective, and biodegradable polymers globally, capable of substituting synthetic materials [2]. Research into biodegradable and innovative products such as cellulose has become crucial because of its distinctive properties. Different methods have been utilized by various researchers to isolate cellulose from agricultural waste or byproducts. However, they generally follow similar sequences of steps in the cellulose isolation process [3]. The order of steps implicated in extraction process were cleansing of raw material to take out dirt particles from it, drying in an oven at normal conditions, grinding to produce powder, using a sieve to achieve the desired particle size, defatting, pretreatment using alkaline, neutralizing it with distilled water, drying, acid treatment, again neutralizing by employing distilled water and drying to obtain the necessary cellulose fibers. Cellulose is typically sourced from various plant components, such as softwood, hardwood, bark, and other plant parts [4].

There is an increasing demand for humans to yield cellulose from farm waste, especially straw, as it can have significant economic value when processed appropriately. In recent years, there has been a transition in cellulose extraction methods from plant-based sources to plant waste sources such as rice straw [5], wheat straw [6], lemon grass straw [4], vetiver straw [7], little millet straw [8], oat straw [9], banana pseudostem [10] and yellow thatching straw [11] etc., many of these cellulose sources are derived from non-wood plants and are not intended for food use. Typically, agricultural waste such as lemon grass straw (referred to as LG after oil extraction) is often burned, but finding appropriate uses for it could alleviate waste disposal challenges. Lemon grass, scientifically known as *Cymbopogan citratus* and belonging to the Poaceae family, is recognized as a significant source of cellulose, hemicellulose, and lignin, comprising approximately 44–45 %, 28–29

* Corresponding author.
** Corresponding author.
E-mail addresses: rafiya.shams@gmail.com (R. Shams), kshirod@tezu.ernet.in (K.K. Dash), kovacsb@agr.unideb.hu (B. Kovács).

https://doi.org/10.1016/j.jafr.2024.101170
Received 18 February 2024; Received in revised form 11 April 2024; Accepted 15 April 2024
Available online 24 April 2024

%, and 17 %, respectively. More than 55 species make up the genus Cymbopogon, with *Cymbopogon flexuosus* and *Cymbopogon citratus* being the primary ones. Currently, *Cymbopogon citratus* is extensively cultivated globally for the extraction of essential oils known for their high citral content (70–80 %) [12]. Extensive utilization of lemon grass plants may lead to the generation of uneconomical biowaste. Consequently, the accumulation of lemon grass leaf biowaste can compromise environmental aesthetics [13]. Composting offers a solution to this waste material, but it may not be a financially efficient approach [14]. Another potential utilization option is the production of pulp and paper, animal feed, textiles, or the use of cellulose as reinforcing material in composites [12].

Lemon grass, belonging to the Gramineae family, is an aromatic grass renowned for its medicinal properties [15]. The leaves of the grass are utilized to pull out LG oil, which exhibits various chemical compositions and finds application in diverse fields such as cosmetics, perfumery, and herbal preparations, owing to its antimicrobial properties [16]. Because lemon grass is readily available, renewable, and biodegradable, cellulose is a great option for creating sustainable material from it [17]. The distinctive features of cellulose obtained from plant remnants, variations may occur depending on the origin of the cellulose source, purification technique, and processing variables, have generated considerable interest in the field. Chemical and mechanical processes are the main ways that cellulose is obtained [18]. The typical approach for extracting cellulose from lingo cellulosic fibers involves a series of steps. The fibers are initially crushed to enhance their surface area. Afterward, they undergo a washing process with double distilled water to eliminate soluble contaminants. Afterward, the fibers undergo treatment with either NaOH or KOH to dissolve the hemicellulose component [19]. Instead of deionized water, alternative solvents like ethanol, benzene, or toluene can be employed for the purpose of separating fatty acids, chlorophyll and phenol based compounds [20]. Subsequently, obtained material is subjected to a bleaching process, This can be achieved using solely NaOH, in conjunction with aqueous H_2O_2, or with $CaClO_2$ or $NaClO_2$ to eliminate any remaining lignin and hemicellulose residues [21].

Microwave heating represents an alternative method for heating that can expedite chemical reactions. This is accomplished through the direct contact among the item undergoing microwave heating and the employed electromagnetic field, resulting in more rapid and volumetric heating compared to traditional heating methods [22]. Furthermore, it offers additional benefits like enhanced selectivity and uniformity, while demanding less energy for the pretreatment of biomass [23]. Microwave-assisted alkaline effect and decolorization lead to cellulose swell and the dissolution of hemicellulose, lignin and various non-cellulosic and non-crystalline contaminants present in corncob. Microwave-assisted chemical treatments, such as alkali treatment and bleaching, reduce hemicellulose and lignin levels, resulting in heightened crystallinity and improved thermal characteristics. The use of microwave irradiation in conjunction with alkali treatment can expedite the chemical reactions accountable for eliminating lignin and breaking down hemicellulose [24]. Microwave heating is a process wherein microwave power directly comes in contact with molecules, inducing quick temperature elevation through electric dipole movement and ion conducting. The fundamental principle of microwaving revolves around rapid movement of hydrophilic molecules, facilitating collisions that transform kinetic energy into heat [25]. Elevated power levels result in higher energy and temperature, which can harm the fibers and give rise to the degradation of lignin [26]. Cellulose holds significant potential for applications in food packaging materials because of its abundant natural sources and unique microstructure and properties. Nonetheless, the intricate hydrogen bonds existing within the cellulose network, both between and within molecules, pose challenges in terms of dissolution and subsequent processing. To tackle this issue, a variety of environmentally friendly solvents have been created. Food packaging films derived from cellulose and produced using these innovative solvent systems exhibit a range of barrier capabilities and outstanding mechanical attributes [27]. The purpose of the present investigation was to isolate cellulose out of lemon grass straw using a chemical applied microwave treatment, it also includes the techno-functional properties and characterization of extracted cellulose.

2. Material and methodology

2.1. Preparation of raw material

Lemon grass (*Cymbopogan citratus*) straw was gathered from the experimental farm during the period of May to June 2023 of Lovely Professional University, Punjab, India. Following sorting and weighing, the straws underwent washing under running water to eliminate dirt and any impurities. Subsequently, they were left at room temperature for one day. To produce lemon grass straw powder (LSP), the straws were placed in stainless steel trays and underwent sun drying at ambient temperatures ranging between 25 ± 5 °C, with a relative humidity of 40 % ± 5, for approximately 3 days. This hybrid drying strategy provides volumetric heating and causes internal vapor generation therefore produces high drying and evaporation rates even at ambient/low temperature range and optimal for removal of moisture which remained during sun drying [22,28].

This process occurred over an average of 9–10 h per day. The dehydrated straws were ground to achieve a consistency that would pass through an 80 mesh sieve, resulting in the production of LSP. To remove the left-over moisture if present the LSP was subjected to an oven drying at 45 ± 5 °C until a constant weight was attained according to Khaerunnisa et al. [29]. The acquired powder was packed into LDPE under ambient storage conditions for straightaway use or packed in aluminum laminated pouches and then stored in a refrigerator at (4 °C) to stop non-significant upsurge in moisture content and water activity throughout storage until analysis was completed [30].

2.2. Methodology for isolation of cellulose from lemon grass straw powder (LSP)

Cellulose fibers were extracted and purified from the dried LSP through microwave-assisted chemical treatment [31,32]. 10 g of LSP was added to 150 mL of varying concentrations of NaOH solution (w/v) and then subjected to microwave heating at different power levels and time combinations (as shown in Table 1). The lemon grass straw pulp procured from this together microwave and alkaline processing was next cleaned and purified thrice with deionized water before neutralization was achieved. Samples were subsequently treated with microwave-assisted decolorization to eliminate any remaining hemicellulose and lignin that may have persisted in the neutralized sample. In this process, the neutralized sample underwent bleaching by immersion into 5 wt% H_2O_2 solution and subsequent microwaving (540 W) for 2 min [31]. Obtained cellulose powder was bleached by soaking it in 5 wt % H_2O_2 at 540 W providing less severe reaction conditions where the chromophore structures in lignin were removed or selectively reacted

Table 1
Treatment table for extraction of cellulose at various power level (W: Watt).

Treatments	Delignification (3min)	Bleaching (2min)
(T1)	180W (4 % NaOH)	540W
(T2)	180W (8 % NaOH)	540W
(T3)	180W (12 % NaOH)	540W
(T4)	360W (4 % NaOH)	540W
(T5)	360W (8 % NaOH)	540W
(T6)	360W (12 % NaOH)	540W
(T7)	540W (4 % NaOH)	540W
(T8)	540W (8 % NaOH)	540W
(T9)	540W (12 % NaOH)	540W
(T10)	720W (4 % NaOH)	540W
(T11)	720W (8 % NaOH)	540W
(T12)	720W (12 % NaOH)	540W

and most of lignin was preserved inhibiting the discoloration by converting primary and secondary alcohols into carbonyl groups through oxidation. This might lead to the dissolution of the impurities containing carboxyl groups, which could then be washed away from the sample [33]. The bleached extract underwent filtration and washing with distilled water unless it reached a neutral pH, after which it was dried at 35 ± 5 °C.

2.3. Characterization of extracted cellulose powder

2.3.1. Yield

The weight of cellulose generated was estimated and yield was evaluated using Equation (1) [34]:

$$\%\ \text{Yield} = \frac{practical\ yield}{Theoritical\ yield} \times 100 \quad (1)$$

2.3.2. pH and solubility

The pH estimation of cellulose solution was conducted employing pH meter by immersing 5 g sample in clean and dried 150 ml beaker containing 40 ml distilled water. After stirring and centrifuge it for 5 min the pH of the supernatant was measured.

Cellulose powder (0.2 g m) extracted was thoroughly mixed in 20 ml 1 % acetic acid solution in a beaker for 30min on a magnetic stirrer at 250rpm at 25 °C. After 30 min of stirring, the solution was filtrated using a 20 μm (μm) nylon membrane filtration assembly. The retardant (insoluble fraction) accumulated on the membrane filter was then washed with deionized water. Cellulose solubility in percentage was calculated by using Equation (2) [34]:

$$\text{Solubility}\% = 100 - \frac{\text{Weight of insoluble fraction}}{\text{Initial weight of the sample}} \times 100 \quad (2)$$

2.3.3. Bulk density, tapped density, hasneur ratio and Carr's index

Approximately 100 mg of cellulose powder was taken in a standard 10 mL measuring cylinder without any thrusting to measure the bulk density, which was defined as milligrams per cubic meter (mg/m^3). For tapped density, 1 g of cellulose powder was taken in a 10 mL standard measuring cylinder, and the contents of the cylinder were gently tapped for 2 min. The ratio of tapped to bulk density provides a measure of flowability and is called as the Hausner ratio as shown in Equation (3) [35]:

$$\text{Hasneur ratio} = \frac{\text{Tapped density (mg/m3)}}{\text{Bulk density (mg/m3)}} \quad (3)$$

Carr's index is the assess of compressibility and is measured via following equation:

$$\text{Carr's index}\ \% = \frac{\text{Tapped density (mg/m3)} - \text{bulk density (mg/m3)}}{\text{Tapped density (mg/m3)}} \times 100 \quad (4)$$

2.3.4. Fourier transform infrared (FTIR) spectroscopy

FTIR (Spectrum 100, PerkinElmer, USA) analysis of prepared cellulose powder was conducted out in order to investigate any alteration in the arrangement of the fibers during the process (Delignification and bleaching). The samples were pulverized and blended with KBr to make pellets, which were subsequently compressed into thin plates for FTIR analysis. FTIR spectra were then noted in the range of 4000–400 cm^{-1}, with a resolution of 4 cm^{-1} [31].

2.3.5. X-ray powder diffractometry (XRD)

XRD analysis of each sample was conducted using Bruker instrument model, D8 Advance (Bruker, Billerica, MA, USA). The particle size was kept up to 200 μm and the diffraction pattern was seen by using Cu-Kα radiations getting 1.54 A° wavelength making angle ranges from 5° to 50°. The crystallinity index (CI) can be studied by applying the Segal equation shown in Eqn. (5) [36].

$$CI = 100 \times \frac{I_{002} - I_{am}}{I_{002}} \quad (5)$$

where I_{002} and I_{am} are the peak intensities at crystalline and amorphous regions correspondingly.

2.3.6. Thermogravimetric analysis (TGA)

The thermal stability of each sample was checked utilizing a thermogravimetric analyzer (Q5000 series, TA Instruments, USA) by heat up samples (about 10 mg) in open alumina pans, under helium atmosphere, from 30 °C up to about 800 °C, at a heating rate of 10 °C/min. Moisture contents (%) were assigned with TGA thermogram using TA Universal Analysis software [37].

2.3.7. Differential scanning calorimetry (DSC)

The thermal particularities of cellulose samples were inspected using DSC, model SDT Q600 from TA Instruments. Samples taken between 10 and 13 mg were made into hermetic pans and carried out from 25 °C to 700 °C at a rate of 5°/min [38].

2.3.8. Statistical analysis

All experiments were done in triplicate, and the outcomes were shown as mean ± standard deviations. Statistical analyses were performed utilizing SPSS software (version 16.0, IBM, Chicago, IL, USA). Mean values were regarded significantly different at the 95 % confidence level ($p < 0.05$).

3. Results and discussion

3.1. Yield and moisture content

The techno-functional characteristics of cellulose powder subjected to various treatments at different power levels were evaluated, and the findings are presented in Table 2. The degree of cellulose extraction, delignification, and hemicellulose hydrolysis are significantly influenced by the treatment parameters such as alkali concentration, extraction duration, and microwave power. While considering the moisture content, the final product exhibited a moisture range of 5.11 %–6.22 %. As illustrated in Table 2, the lemon grass straw powder yield, following different treatments, ranged from 33.11 % to 37.46 %. The ultimate dry weight of the powder along with maximum yield was most substantial for treatment T8, employing a power level of 540 W with 8 % NaOH, and lowest yield for treatment T1, utilizing a power level of 180 W with 4 % NaOH. Klunklin et al. [39] and Louis et al. [40] noted a comparable pattern when examining the influence of NaOH concentration on cellulose yield. Elevated concentration of NaOH is known to facilitate lignin dissolution, leading to a proportional increase in lignin removal [41]. Mohamad et al. [42] also reported a similar influence on cellulose yield. This finding highlighted that the influence of NaOH concentration plays a crucial role in deciding whether the extraction process will prioritize high lignin removal or yield a higher pulp quantity. Regarding various microwave power levels, the rise in watts corresponds to an increase in temperature, potentially resulting in even mixing of microwave energy. This phenomenon may result in the breakdown of ether and ester linkages within the lignin-carbohydrate complicated structure of fiber. This suggests a potential arrangement of cellulosic chains, consistent with findings previously described by Ahmed et al. [43], Wang et al. [44] and Liu et al. [45]. Above results elucidated that the refining pretreatment resulted in the extraction and separation of hemicelluloses with elevated molecular weights during the microwave and alkaline treatment combination.

Table 2
Techno-functional properties of prepared cellulose samples.

S. No.	Cellulose sample	Moisture %	Yield %	pH	% Solubility	Bulk density	Tapped density	Carr's index	Hasneur ratio
1.	T1 (180W,4 %)	5.45 ± 0.07	33.26 ± 0.25	5.9 ± 0.17	40 ± 0.15	0.32 ± 0.03	0.40 ± 0.17	20 ± 5.56	1.25 ± 0.05
2.	T2 (180W,8 %)	5.29 ± 0.04	35.28 ± 0.31	6.1 ± 0.15	40 ± 0.75	0.31 ± 0.03	0.39 ± 0.03	20.51 ± 5.71	1.25 ± 0.08
3.	T3 (180W,12 %)	5.21 ± 0.03	33.11 ± 0.45	6.5 ± 0.17	40 ± 0.26	0.31 ± 0.02	0.36 ± 0.02	13.88 ± 0.15	1.16 ± 0.08
4.	T4 (360W,4 %)	5.24 ± 0.08	34.73 ± 0.21	6.1 ± 0.17	40 ± 0.09	0.29 ± 0.02	0.34 ± 0.06	14.70 ± 0.13	1.17 ± 0.07
5.	T5 (360W,8 %)	5.17 ± 0.03	36.19 ± 0.11	6.4 ± 0.15	40 ± 0.17	0.36 ± 0.03	0.43 ± 0.04	16.27 ± 0.11	1.19 ± 0.07
6.	T6 (360W,12 %)	5.05 ± 0.04	34.81 ± 0.06	6.8 ± 0.1	45 ± 0.22	0.36 ± 0.03	0.42 ± 0.05	14.28 ± 0.21	1.16 ± 0.08
7.	T7 (540W,4 %)	6.22 ± 0.03	36.82 ± 0.24	6.9 ± 0.1	40 ± 0.11	0.39 ± 0.01	0.46 ± 0.05	15.21 ± 0.59	1.17 ± 0.10
8.	T8 (540W,8 %)	5.27 ± 0.02	37.46 ± 0.09	7.2 ± 0.1	55 ± 0.46	0.37 ± 0.02	0.42 ± 0.05	11.90 ± 0.43	1.13 ± 0.05
9.	T9 (540W,12 %)	5.11 ± 0.10	36.51 ± 0.144	7.4 ± 0.1	55 ± 0.21	0.32 ± 0.03	0.39 ± 0.03	17.94 ± 0.94	1.21 ± 0.07
10	T10 (720W,4 %)	6.18 ± 0.24	36.18 ± 1.15	5.6 ± 0.1	35 ± 0.61	0.33 ± 0.05	0.41 ± 0.06	19.51 ± 0.69	1.24 ± 0.12
11	T11 (720W,8 %)	6.02 ± 0.15	35.21 ± 0.23	5.9 ± 0.1	35 ± 0.02	0.31 ± 0.04	0.45 ± 0.06	20 ± 4.32	1.25 ± 0.13
12	T12 (720W,12 %)	5.69 ± 0.12	36.01 ± 0.06	6.1 ± 0.14	35 ± 0.13	0.31 ± 0.03	0.37 ± 0.05	16.21 ± 0.21	1.19 ± 0.06

3.2. Flow properties of lemon grass straw cellulose

Bulk density offers a prediction of a material's flowability, whereas tap density assesses the efficiency with which a powder can be densely packed into a compact area through persistent tapping. In broad terms, elevated bulk and tapped densities suggest enhanced possibility for material flow and reorganization under compaction [46]. Carr's compressibility and Hausner indices were computed as ratios indicating the disparity among tapped and bulk densities. Carr's compressibility index confers a conception of a powder's compressibility, indicating its compressibility level, whereas the Hausner index evaluates the cohesion among particles. Regarding Carr's index, values falling within the ranges of 5–10, 11–15, 16–20, and 21–25 signify excellent, good, fair, and poor flow nature of the material, correspondingly [47]. Conversely, in case of Hausner ratio, value below 1.20 indicate favorable flowability, while a value of 1.50 or above reveals poor flow properties for the sample. According to the findings of this research, the cellulose extracted at 540 W using 8 % NaOH exhibited a Carr's index of 11.90, indicating good or free-flowing properties. The Hausner ratio was 1.13, falling below 1.25 (indicating good flowability), further confirming its favorable flow characteristics in comparison to the commercial cellulose displayed a Carr's index of 21.05 % and a Hausner ratio of 1.25 ± 0.04. The favorable flow characteristics observed in cellulose are likely attributed to differences in particle shape, size, and surface area among the powders. Hence, the values recorded for the Hausner ratio align with those of the Carr's index. Comparable outcomes can be correlated with the findings reported by Duruaku et al. [46], Sundarraj et al. [48], and Parid et al. [49]. Examining the impact of alkaline concentration, it was noted that the concentration of alkali had a substantial positive effect on both Carr's index and Hausner's ratio at $p < 0.01$, while demonstrating a notable adverse effect on porosity at $p < 0.01$ [50]. This could be attributed to the lower concentration of sodium hydroxide, which may lessen the hydrogen bonds present within the cellulose chain to a lesser degree potentially leading to a lesser change in bulk and tapped density, as suggested by Tasnim et al. [51]. The changes in the flow characteristics of the extracted cellulose could be attributed to differences in particle size, shape, and surface texture, which are influenced by varying alkali concentration, as noted by Tasnim et al. [51]. Moreover, the hydrogen bonds present within the cellulose are debilitated or broken at lower temperatures in the existence of sodium hydroxide, increasing the likelihood of correlation between cellulose and water molecules. Consequently, the cellulose chain may experience dissolution in water, a process dependent on factors such as molecular weight, temperature, and the strength of sodium hydroxide, as indicated by Ref. [52].

3.3. pH and solubility

Rheological properties can serve as indicators with a profound influence on the final dry product. While there has been limited focus on the solution state and rheological properties before precipitation, these properties are crucial in identifying specific factors that could contribute to mechanical properties [53]. As per the United States Pharmacopoeia (2004) and the British Pharmacopoeia (2004), cellulose is expected to have a pH within the range of 5–7. The pH of the microcrystalline cellulose samples prepared in this study is 7.2, which falls within the acceptable range for standard cellulose. It is noteworthy that the commercial-grade cellulose sample, commonly claimed as an excipient in the pharmaceutical industry, exhibits a pH similar to that of the prepared cellulose samples, as indicated in the table [52]. Cellulose is notably amphiphilic, and its limited solubility in water is primarily attributed to hydrophobic interactions. Additionally, the solubility of cellulose in water becomes more pronounced at extreme pH values, as highlighted by Lindman et al. [54]. Various cellulose derivatives, like methyl cellulose or hydroxyethyl cellulose, can exhibit high water solubility despite possessing a considerable capacity for intermolecular hydrogen bonding, often comparable to that of cellulose itself [55].

Concerning the solubleness of cellulose, it is commonly acknowledged that cellulose is challenging to go into solution, with only a less range of solvents present. A significant period of exploration occurred in 1930s, during which four major types of solvents were found and are still under study today: phosphoric acid, NaOH–water, ionic liquids, and amine oxides, as outlined by Budtova et al. [56]. The solubleness of cellulose is not specified by macroscopic characteristics like fiber dimensions, but prefer being properties existing at micro and nano scales, but by qualities at the micro and nano levels, specifically in regions proximate to the molecular and supramolecular structure of cellulose within fibrils and fibril sums in the cell wall, as discussed by Kihlman et al. [57]. According to the data in the table, treatment T8, conducted at 540 W using 8 % NaOH, exhibited the highest solubility. This result may be attributed to the fact that solubility tends to increase as the chain length of cellulose decreases. Extreme pH levels, whether excessively low or high, can adversely affect the chain unit of the cellulose polymer, leading to potential breakage of the *N*-glycosidic bonds within the anhydroglucose polymer [55,55]. A survey led by Swensson et al. [58] highlighted that the combination of NaOH with tetra-methyl ammonium hydroxide exhibited combined consequence on cellulose dissolving and proved to be a more effective solvent for cellulose compared to mixture of NaOH with benzyl tri-methyl ammonium hydroxide. This finding underscores the importance of carefully selecting the base pair to enhance the dissolution capacity of cellulose solutions, despite the individual superior dissolution ability of benzyl tri-methyl ammonium hydroxide. An alternative method to enhance solubility involves the addition of co-solutes. Co-solutes can diminish hydrophobic interactions, thereby enhancing aqueous solubility. Examples include urea and its derivatives and polyethylene glycol (PEG) [54]. Another crucial factor influencing the improved solubility of cellulose is temperature. At lower temperatures, there is a preference for higher polar configuration around the C–C bonds, facilitating strong positive interactions with a polar solvent. With increasing temperature, less polar configuration tends to increasingly predominant [59]. Elevated temperature induces

phase separation, commonly observed as a "clouding" effect, which is prevalent across various nonionic polymers and most nonionic surfactants. This phenomenon can be ascribed to conformational changes that render polymer chains little polar at extreme temperatures [60].

3.4. Fourier transform infrared (FTIR) spectroscopy

Fourier-transform infrared spectroscopy (FTIR) is an effective method of analysis that is utilized in characterizing the chemical nature of materials, such as cellulose obtained through microwave-assisted extraction (MAE). As the sample was exposed to infrared light, it interacted with the molecular bonds in the cellulose, resulting in the absorption of certain wavelengths that were characteristic to the substance. The FTIR spectrum yielded data regarding the functional groups that exist in the cellulose sample. The spectrum of cellulose exhibited distinct peaks that correspond to the vibrations of specific functional groups, involving hydroxyl (OH), carbonyl (C=O), and glycosidic linkage (C–O–C), inside the cellulose polymer chain. Existence of wide peak between 3300 and 3600 cm^{-1} displays the occurrence of O–H stretching vibrations originating from the hydroxyl groups of cellulose. The peaks noted in the range of 2800–3000 cm^{-1} agrees to the stretching of C–H bonds in cellulose structure. The existence of absorbed moisture was indicated by the peak seen at nearly 1630-1640 cm^{-1}. The peaks observed in the range of 1000–1200 cm^{-1} are denotative of C–O and C–C stretching vibration in the cellulose substrate. The characteristic peaks if appeared at ~1500 cm^{-1} in extracted cellulose powder may be nominated to this C=C stretching. Absence of these peaks in the spectra is because of partial exclusion of residual hemicellulose and lignin [61]. FTIR analysis enabled the identification and confirmation of cellulose's existence, while also offering valuable information regarding its structural characteristics, including crystallinity, polymerization degree, and chemical alterations. By analyzing the FTIR spectra of cellulose extracted using different combinations of microwave power levels and extraction times, variations have been observed in both the purity and structural integrity of the extracted cellulose. The FTIR peaks and their intensities were subject to variation depending on the microwave power level and extraction time used for the extraction process. Hence, FTIR serves as a beneficial technique for both qualitative and quantitative evaluation of cellulose acquired by microwave-assisted extraction at different power level and extraction time.

The characteristic absorption peaks of T2 were detected at the wavenumbers 573 cm^{-1}, 1029 cm^{-1}, 1234 cm^{-1}, 1375 cm^{-1}, 1551 cm^{-1}, 1634 cm^{-1}, 2916 cm^{-1} and 3268 cm^{-1} while the T5 showed the absorption peaks at 553 cm^{-1}, 1033 cm^{-1}, 1374 cm^{-1}, 1628 cm^{-1}, 2361 cm^{-1} and 3264 cm^{-1}. There were characteristic absorption peaks of T8 at the wavenumbers of 564 cm^{-1}, 1026 cm^{-1}, 1313 cm^{-1}, 1375 cm^{-1}, 1548 cm^{-1}, 1630 cm^{-1}, 2360 cm^{-1}, 2960 cm^{-1}, 2917 cm^{-1} and 3274 cm^{-1}. The new absorption peak at the wavenumber (2960-2361) cm^{-1} was observed whereas the absorption peaks at (2916–2917) cm^{-1} in the T2 and T8 were not observed as for T5 samples. The absorption peaks at (1548–1551) cm^{-1} observed in all the remaining two samples (T2 and T8) were not observed in the T5 sample where T2, T5 and T8 represents delignification at 180 W using 8 % NaOH, 360 W using 8 % NaOH) and 540 W using 12 % NaOH. From the FTIR analysis shown in Figure. (1) it was observed that T8 showed the maximum absorption peaks and the peak intensities compared to the remaining samples where T5 showed the lowest peak intensities. This observation suggested that the microwave-assisted extraction of cellulose greatly affected the intra and inter-molecular bonding structures in the case of T5 while T8 showed the least affected one.

The characterization of cellulose with FTIR yielded results similar to those obtained in the studies conducted earlier where cellulose showed the main peak at 3367 cm^{-1} which lies in the range of 3000–3600 cm^{-1} in the spectra is because of the O–H stretching [62]. Furthermore, water molecules can establish hydrogen bonds with adjacent molecules, exhibiting a range of bond lengths and stretching vibrational

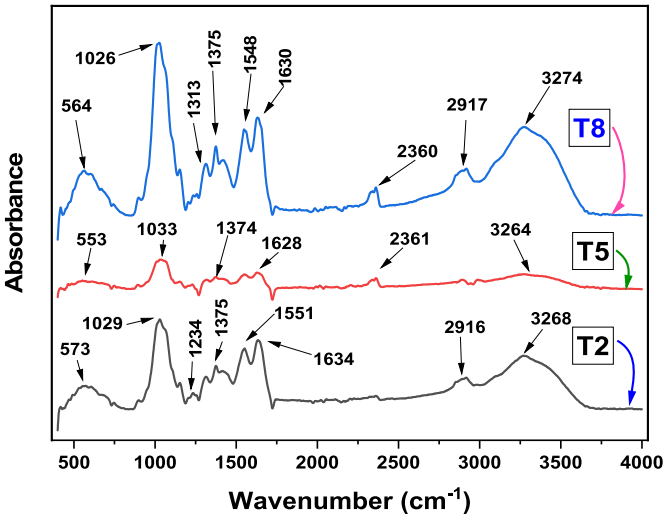

Fig. 1. The FTIR spectra of cellulose samples obtained through various treatments.

frequencies. This leads to the OH functional groups of water producing continuous vibrational frequencies, resulting in a significantly broad and predominant infrared absorption within the hydrogen bonding region of 3000–3700 cm^{-1}. However, another study showed the wide absorption bands ranging from 3650 cm^{-1} to 3200 cm^{-1}signify the existence of hydrogen-bonded hydroxyl groups within their structure upon extracting cellulose fibrils from rice husk [63]. Conversely, the absorption band observed near ~1370 cm^{-1} in FTIR spectra is ascribed to C–H bending. Studies have indicated that the band in this region exhibits the most notable distinctions between crystalline cellulose II and amorphous cellulose. Subsequently, it was shown that these bands were not specific to the amorphous regions [64]. In another IR spectra of the cellulose flakes of olive husk. Transmittance peaks at 1433, 1378, and 1315 cm^{-1}, in according to bending vibrations of -CH_2, C–H, and C–O of cellulose, were identified in the spectra of extracted cellulose from olive husk [65]. The peaks and intensities seen in lemon grass straw cellulose varied slightly depending on the treatment applied, which can be approved to disparity in molecular structures and extraction conditions used.

3.5. X-ray powder diffractometry (XRD)

The structural characteristics of cellulose extracted by microwave-assisted extraction (MAE) at different power levels and time combinations were reviewed utilizing X-ray diffraction (XRD) and presented in Figure (2). X-ray diffraction (XRD) is a method given to assay the crystalline structure of cellulose. It provided precise details regarding the degree of crystallinity, the size of the crystals, and their arrangement. Cellulose Iα and Iβ phases were encountered in cellulose of lemon grass. The diffraction pattern that emerges is a sequence of peaks that directly correspond to the organization of atoms or planes within the crystalline structure of cellulose. The presence of distinct peaks at various angles in crystalline cellulose enabled the identification of the direction and intensity of its crystalline structure. The predominant type of cellulose, known as Cellulose I displayed peaks at around $2\theta = 14.8°$, 16.5°, and 22.5°. The degree of crystallinity was determined by comparing the intensity of the crystalline peaks with that of the amorphous base. The XRD analysis of cellulose produced using microwave-assisted extraction revealed the crystalline characteristics of the extracted cellulose. An analysis was conducted to evaluate the efficacy of MAE in maintaining or altering the crystalline structure of cellulose under different power levels and durations. The characteristic X-ray diffraction peaks were observed at the 2θ of 19.0° and 26.6° for T2, 19.3°, 26.7° and 68.2° for

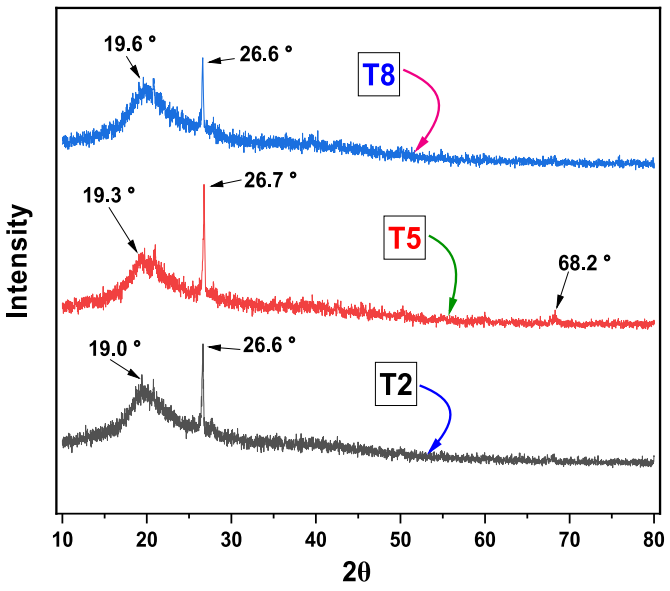

Fig. 2. Diffractogram of cellulose samples obtained through various treatments.

T5 and at 19.6° and 26.6° for T8 samples. The broad peak at (19.0–19.6°) could be as assigned as the amorphous nature of the polysaccharide (cellulose). The more crystalline peaks and higher peak intensity at 2θ values of 26.7° indicated the greater crystallinity of the T5 samples. The T8 sample showed the lowest crystalline peak (at 2θ value of 26.6°) intensity signifying the lowest crystalline character. Thus, the XRD analysis demonstrated that the T5 samples exhibited the highest crystalline character while the T8 sample was the lowest during the microwave-assisted extraction of cellulose.

The crystallinity index (CI) was suggested subsequent the method outlined by Segal equation as mentioned by Ref. [66] offering a quantitative assessment of crystallinity in powders and its correlation with the strength and hardness of fibers [67]. As indicated in Table 2, the values of the crystallinity index were 65.54 %, 68.88 % and 70.02 % for treatment T2, T5 and T8. The observed rise in crystallinity in the treated samples can be awarded to the expulsion of removal of hemicellulose and lignin from the amorphous regions during microwaving with chemical treatments. Microwave-assisted treatments alleviate force prevailing between the crystalline part of cellulose and other non-cellulosic components within the cell wall (hemicellulose and lignin) [68]. The rise in crystallinity percentage enhances the rigidity of cellulose, while the intensity of hydrogen bonds (HBI) is inversely correlated with crystallinity. A rise in HBI indicates heightened hydrogen bonding among specific hydroxyl functions in cellulose, commonly observed during the shift from cellulose I to cellulose II, despite resulting in a decrease in the overall crystallinity index [64]. The elevated percentage of crystallinity in the treated samples signifies a well-organized and densely packed molecular structure, suggesting that the resultant cellulose polymer possesses a significant crystal area in contrast to amorphous region. This characteristic enhances its strength and renders it suitable as a raw material for packaging applications [37]. Consequently, fibers acquired by means of microwave-assisted chemical treatments are poised to significantly enhance mechanical characteristics in composite materials, primarily because of heightened Young's modulus in the crystalline region along the longitudinal direction [69]. Various treatment parameters did certainly influence the crystal structure of cellulose, primarily associated with alterations in the crystal lattice.

Lin et al. [70] extracted cellulose from bamboo showed three typical peaks at 34.66°, 21.62° and 15.93° in the diffraction pattern of cellulose I but also showed a shoulder around 19.86° and three additional peaks at 16.54°, 14.76°, 12.08°. These peaks belong to the cellulose II. The increase in diffraction angle was attributed to the decrease in d-spacing of planes, as per the Bragg equation, indicating that cellulose experienced an enlargement in breakage strain and a fall in Young's modulus. In a separate study, cellulose fibers were isolated from rice husk, and researchers noted a distinct crystalline peak at a 2θ diffraction angle of 22.5°, as there was no doublet in the intensity of the main peak corresponding to Cellulose-I polymorph, again which implies higher crystallinity is due to effective elimination of noncellulosic components [71]. Another study carried out by Abdullah et al. [72] where the XRD diffractogram shows the X-ray diffraction pattern of coconut husk microcrystalline cellulose exhibits the highest peaks at intensities of 2θ of 23°, 15° and 12° and the degree of crystallinity composed in this study was 71.8 % suggesting that the resultant cellulose polymer possesses a substantial crystalline area in contrast to the amorphous region, thereby enhancing its strength and rendering it valuable as a raw material for packaging. Similar diffraction peaks were observed when cellulosic fibers excavated from the roots of the *Acalypha indica* L. plant exhibited the Iβ type, which represents the allotropic form of cellulose and contributes to its rigid nature. The X-ray diffractogram revealed a distinct pointed peak at 2θ = 22.48°, indicating the presence of crystalline cellulose I, while a less pronounced and lower density peak was observed at 2θ = 16.16°, suggesting the existence of the amorphous component of cellulose. The crystalline index of the fibers was determined to be 46.62 % using the Segal peak height method [73]. Akinjokun et al. [74] also reported comparable findings from the excavation of cellulose nanocrystals from cocoa pod husk the most significant peaks observed at 15.97°, 22.63°, and 34.63° at 2θ angles in the X-ray diffractogram correspond to the crystallographic planes typically associated with the cellulose I polymorph structure, indicating the presence of the characteristic cellulose I structure. Furthermore, the narrow peak at 2θ = 22.63° is attributed to the decomposition of the amorphous hemicelluloses and lignin components. The after revival of the crystalline part of the fiber led to the appearance of potent and more restricted peaks in the diffractogram.

3.6. Thermogravimetric analysis (TGA)

The thermal characteristics of materials, including cellulose extracted by microwave-assisted extraction (MAE), were investigated using the thermogravimetric analysis (TGA) technique and shown in Figure (3). Thermogravimetric analysis (TGA) quantifies the variation in

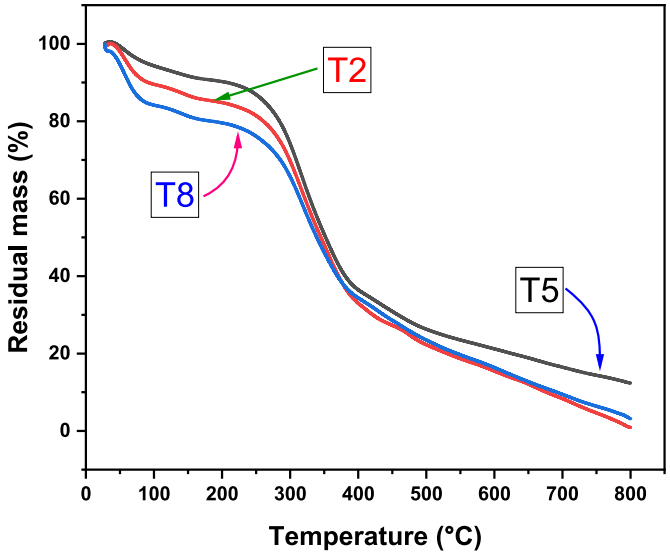

Fig. 3. The thermogravimetric analysis of cellulose samples obtained through various treatments.

mass of a substance with respect to temperature, offering valuable information on its resistance to heat, disintegration, and chemical composition. The TGA curve displayed the relationship between weight loss and temperature over time. Cellulose displayed a curve with numerous stages of weight loss, which was attributed to various degradation processes. The earliest loss in weight (up to 100 °C) was ascribed to elimination of moisture that was either adsorbed or bound. Additional reduction in weight was seen within the temperature reach of 200–350 °C, which amounts to the breakdown of hemicellulose, cellulose, and other organic constituents. The residual substance remaining after the degradation consisted of cellulose char and several inorganic substances. TGA analysis facilitated the assessment of the thermal stability and breakdown characteristics of cellulose obtained via MAE under different combinations of microwave power and time. This study facilitated the comparison of the thermal properties of cellulose obtained through various extraction methods and provided insights into the influence of microwave-assisted extraction on the thermal degradation parameters of cellulose. Having knowledge of the thermal constancy of the extracted cellulose is vital for evaluating its applicability for different applications.

The TGA thermogram shows three thermal degradation stages. The first stage occurred below 177 °C which may be accredited to the moisture/water loss. The second stage occurred between 203 and 540 °C which might be due to the high temperature degradation of polysaccharides i.e., cellulose. The third stage began from 540 °C that could have assigned to carbonization of the inorganic compounds. In the stage, the T2 sample showed a thermal loss of 14.2 %, 9.4 % for T5 and 19.55 for T8 samples. A mass loss of 64.2 %, 65.9 % and 60.2 % were observed for T2, T5 and T8, respectively in the I the second stage. The residual mass of 3.2 %, 12.4 % and 0.9 % were observed for the T2, T5 and T8 samples respective in the third stage of thermal degradation. Therefore, the TGA analysis proved that the T5 samples exhibited the greatest thermal stability in contrary to the other samples.

The findings obtained are uniform with the results by Sahu et al. [75] upon extracting cellulose from natural *Cascabela Thevetia* bast fibers and reported Degradation initiates around 30 °C for all fibers, imputed to the existing trapped moisture particles that evaporate amid the heating process. The initial decomposition temperature of treated fibers was observed to fall within 250–270 °C range, resulting in of 8–15 % weight loss, while the final decomposition temperature of all treated fibers resides within the range of 390–450 °C, accompanied by a weight loss of 48–55 %. Similarly, cellulose when extracted from olive husk showed the initial mass loss at 30–100 °C with weight deduction of less than 5 %. which is because of evaporation. The thermal breakdown of hemicellulose was linked to a moderate thermal peak occurring at 200–300 °C, resulting in a weight reduction of 46.13 %. The thermal degradation of cellulose led to a notable peak temperature ranging approximately from 320 to 400 °C. Ash formation occurred at temperatures exceeding 700 °C. Due to robust phenolic-binding interactions, the findings indicated that olive husk fibers could withstand high temperatures [37]. In another study cellulose was extracted from Klaai et al. [65] the extracted cellulose shows the similar thermogram from olive husk as in our study. Here The initial phase, which takes place within the range of 70–100 °C, is characterized by the water loss amounting to approximately 7.48 %. The second stage of thermal degradation occurs at approximately 211 °C, attributed to the decomposition of hemicellulose and cellulose. The third decomposition event is attributed to the decomposition of lignin at approximately 343 °C. Nonetheless, a slight weight loss of approximately 5.13 % around 100 °C complies to moisture evaporation. The next decomposition temperature begins at 221 °C and continues up to 370 °C. During this stage, cellulose undergoes degradation, resulting in the production of hydrocellulose and levo-glucosan. The TGA results of untreated fibers from another study indicate that peak values commence between 40 and 80 °C, with the onset of decomposition reaching 260 °C, providing clear evidence of enhanced fiber thermal stability under experimental conditions. In the second stage, the cellulose within the fiber initiates combustion by reason of existence of covalent bonds between the cellulose and fiber materials. Furthermore, the onset of mass loss at 250 °C for the second peak, as indicated by the TGA curve, is a noteworthy property of the fiber, which makes it suitable for high-temperature applications in structural materials.

3.7. Differential scanning calorimetry (DSC)

Differential scanning calorimetry (DSC) is a process of thermal investigation that examines the heat flow connected with material transitions in relation to temperature changes. Differential scanning calorimetry (DSC) was utilized to examine the thermal characteristics of cellulose obtained through microwave-assisted extraction (MAE). The resultant DSC curve exhibited peaks or troughs that corresponded to distinct heat reactions taking place within the cellulose sample are shown in Figure (4). Cellulose, an example of amorphous materials, demonstrated a glass transition temperature, which corresponded to a shift in its physical characteristics caused by enhanced molecular mobility. Cellulose exhibited distinct peaks related to melting or crystallization, particularly in samples with higher levels of crystallinity. Endothermic peaks were identified, indicating the absorption of energy during processes associated to decomposition or thermal degradation. Differential scanning calorimetry (DSC) study revealed insights into the thermal transitions and characteristics of cellulose derived via microwave-assisted extraction (MAE). The study provided insights into the outcome of microwave-assisted extrication on the thermal characteristics of extracted cellulose, including crystallization, melting behavior, and thermal stability. The findings derived from DSC analysis, when combined with other characterization techniques, enhanced our extensive comprehension of the thermal properties and appropriateness of cellulose extracted through MAE for diverse applications in food and pharmaceutical industries. The DSC analysis of the T2 samples showed To, Tm, Tc and ΔH values as 52.4 °C, 75.7 °C, 96.3 °C and 0.011 J/g, respectively. The To, Tm, Tc and ΔH of the T5 sample were 55.1 °C, 75.1 °C, 125.1 °C and 0.040 J/g while the values for T8 sample were 53.9 °C, 69.2 °C, 88.7 °C and 0.015 J/g, respectively. The higher Tm and ΔH of the T5 sample demonstrated improved thermal properties compared to the T2 and T8 samples.

4. Conclusion

Depending on the conducted characterization studies, it can be inferred that the straws of *Cymbopogan citratus* exhibit significant

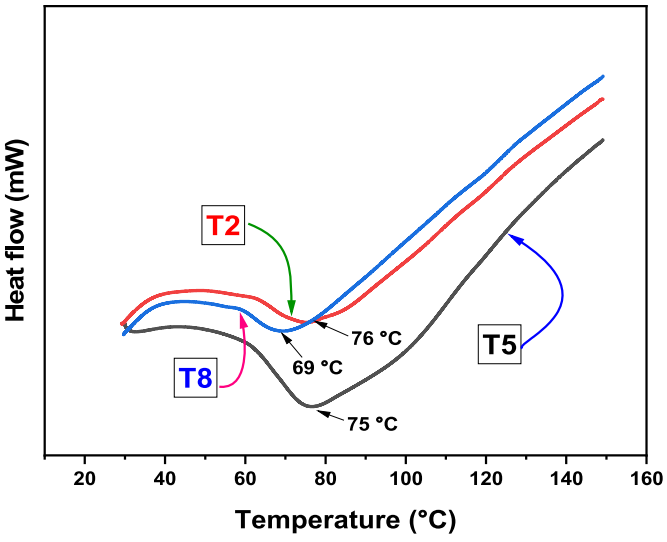

Fig. 4. Differential scanning calorimetry (DSC) of cellulose samples obtained through various treatments.

characteristics that render them suitable for the production of eco-friendly composites. In the conventional method, the alkali solution typically needs to be heated for 2–4 h to effectively remove lignin and hemicellulose. However, employing microwave treatment reduces the processing time to just a few minutes. This method represents a significantly more effective and environmentally affable method for synthesizing cellulose from lemon grass straw. In this method, we have also reduced the bleaching process time from hours to just minutes. The microwave-assisted chemical treatment entailed upsurge in the crystallinity of cellulose, reaching up to 70.02 %. The thermal conduct of the fibers suggests that they can be utilized in environments where implying temperatures are under 200 °C, attributed to their higher crystallinity. The FTIR spectral analysis affirms the effective removal of wax, lignin, and hemicelluloses from the fiber surface. Composite materials depending upon natural fibers are environmentally preferable and find application in a wide array of products, like automotive components, aerospace parts, ceiling panels, packaging materials, and more. Despite the rapid depletion of forests worldwide, there is still a growing demand for wood products. In the realm of green technology, endeavors are underway to develop wood substitutes that combine wood materials with polymers to produce cost-effective, high-performance, and termite-resistant products. Therefore, the findings of this study indicate that cellulose derived from lemon grass straw could serve as a viable substitute raw material for use as an innate reinforcement in biofilms and biocomposites. Additionally, research in this area could explore new opportunities for creating eco-friendly composites across various applications, emphasizing sustainability. The cellulose isolated from lemon grass straw represents a novel source of environmentally friendly material suitable for use in polymer composite applications. Furthermore, these findings underscore the potential for profitable utilization of agricultural residue in cellulose production, thereby contributing to a significant economic activity.

Funding

Funding Project No. TKP2021-NKTA-32 has been implemented with support from the National Research, Development and Innovation Fund of Hungary, financed under the TKP2021-NKTA funding scheme, and supported by the University of Debrecen Program for Scientific Publication.

CRediT authorship contribution statement

Adity Bahndral: Data curation, Formal analysis, Investigation, Methodology, Project administration, Resources, Software, Validation, Visualization, Writing – original draft. **Rafeeya Shams:** Conceptualization, Data curation, Formal analysis, Investigation, Methodology, Project administration, Resources, Software, Supervision, Validation, Visualization, Writing – review & editing. **Kshirod Kumar Dash:** Writing – review & editing, Writing – original draft, Visualization, Conceptualization, Data curation, Formal analysis, Funding acquisition, Investigation, Methodology, Project administration, Resources, Software, Supervision, Validation. **N. Afzal Ali:** Visualization, Validation, Software, Methodology, Formal analysis. **Ayaz Mukarram Shaikh:** Formal analysis, Funding acquisition, Resources, Software, Validation, Visualization. **Béla Kovács:** Funding acquisition, Project administration, Resources, Software, Validation, Visualization.

Declaration of competing interest

The authors declare that they have no known competing financial interests or personal relationships that could have appeared to influence the work reported in this paper.

Data availability

Data will be made available on request.

References

[1] B. Koul, M. Yakoob, M.P. Shah, Agricultural waste management strategies for environmental sustainability, Environ. Res. 206 (2022) 112285, https://doi.org/10.1016/j.envres.2021.112285.
[2] R. Khan, R. Jolly, T. Fatima, M. Shakir, Extraction processes for deriving cellulose: a comprehensive review on green approaches, Polym. Adv. Technol. 33 (2022) 2069–2090, https://doi.org/10.1002/pat.5678.
[3] S. Banerjee, A. Arora, Biovalorization of agricultural wastes for production of industrial enzymes, in: Value-Addition in Agri-Food Industry Waste through Enzyme Technology, Academic Press, 2023, pp. 107–122.
[4] 1229-1233 ©. Tpi, Studies on effect of different process parameters on, (n.d.). https://www.thepharmajournal.com/archives/2023/vol12issue4/PartN/12-4-125-909.pdf (accessed February 28, 2024).
[5] V.W.X. Lai, J. Jamaluddin, N.A.F. Mat Nasir, N. Baharulrazi, R.A. Majid, J.C. Lai, S. P. Mohd Bohari, L.S. Chua, R. Hasham, Z. Rahmat, N. Adrus, Extraction of cellulose from rice straw for regeneration of hydrogels, Environ. Qual. Manag. (2021), https://doi.org/10.1002/tqem.21825.
[6] Q. Liu, W.-Q. He, M. Aguedo, X. Xia, W.-B. Bai, Y.-Y. Dong, J.-Q. Song, A. Richel, D. Goffin, Microwave-assisted alkali hydrolysis for cellulose isolation from wheat straw: influence of reaction conditions and non-thermal effects of microwave, Carbohydr. Polym. 253 (2021) 117170, https://doi.org/10.1016/j.carbpol.2020.117170.
[7] R. Seth, A. Meena, R. Meena, Enzyme-based green synthesis, characterisation, and toxicity studies of cellulose nanocrystals/fibres produced from the Vetiveria zizanioides roots agro-waste, Environ. Sci. Pollut. Res. Int. (2022), https://doi.org/10.1007/s11356-022-24455-x.
[8] C.M. Dominic, V. Raj, K.V. Neenu, P.S. Begum, K. Formela, M.R. Saeb, J. Parameswaranpillai, Chlorine-free extraction and structural characterization of cellulose nanofibers from waste husk of millet (Pennisetum glaucum), Int. J. Biol. Macromol. 206 (2022) 92–104.
[9] N. Sjöstedt, Isolation of Cellulose Fibres from Agricultural Waste. Production of Dissolving-Grade Pulp from Oat Husk and Wheat Straw, 2022.
[10] G. Zope, A. Goswami, S. Kulkarni, Isolation and characterization of cellulose nanocrystals produced by acid hydrolysis from banana pseudostem, Bionanoscience 12 (2022) 463–471, https://doi.org/10.1007/s12668-022-00960-8.
[11] N. Ndwandwa, F. Ayaa, S.A. Iwarere, M.O. Daramola, J.B. Kirabira, Extraction and characterization of cellulose nanofibers from yellow thatching grass (Hyparrhenia filipendula) straws via acid hydrolysis, Waste Biomass Valorization 14 (2023) 2599–2608, https://doi.org/10.1007/s12649-022-02014-2.
[12] V. Fiore, D. Badagliacco, C. Sanfilippo, R. Pirrone, S. Siengchin, S.M. Rangappa, L. Botta, Lemongrass plant as potential sources of reinforcement for biocomposites: a preliminary experimental comparison between leaf and culm fibers, J. Polym. Environ. 30 (2022) 4726–4737, https://doi.org/10.1007/s10924-022-02545-8.
[13] R. Zein, J. Satrio Purnomo, P. Ramadhani, Safni, M.F. Alif, C.N. Putri, Enhancing sorption capacity of methylene blue dye using solid waste of lemongrass biosorbent by modification method, Arab. J. Chem. 16 (2023) 104480, https://doi.org/10.1016/j.arabjc.2022.104480.
[14] S. Marcelino, P.D. Gaspar, A. Paço, Sustainable waste management in the production of medicinal and aromatic plants—a systematic review, Sustainability 15 (2023) 13333, https://doi.org/10.3390/su151813333.
[15] R. Patel, LEMONGRASS-A BOON to mankind, Int. J. Inf. Futur. Innovat. Eng. 2 (2023) 192–205.
[16] A.C. Kumoro, D.H. Wardhani, D.S. Retnowati, K. Haryani, A brief review on the characteristics, extraction and potential industrial applications of citronella grass (Cymbopogon nardus) and lemongrass (Cymbopogon citratus) essential oils, IOP Conf. Ser. Mater. Sci. Eng. 1053 (2021) 012118, https://doi.org/10.1088/1757-899x/1053/1/012118.
[17] P. Kumari, G. Pathak, R. Gupta, D. Sharma, A. Meena, Cellulose nanofibers from lignocellulosic biomass of lemongrass using enzymatic hydrolysis: characterization and cytotoxicity assessment, Daru 27 (2019) 683–693, https://doi.org/10.1007/s40199-019-00303-1.
[18] C.C. Hernandez, F.F. Ferreira, D.S. Rosa, X-ray powder diffraction and other analyses of cellulose nanocrystals obtained from corn straw by chemical treatments, Carbohydr. Polym. 193 (2018) 39–44, https://doi.org/10.1016/j.carbpol.2018.03.085.
[19] Y. Xie, X. Guo, Z. Ma, J. Gong, H. Wang, Y. Lv, Efficient extraction and structural characterization of hemicellulose from sugarcane bagasse pith, Polymers 12 (2020) 608, https://doi.org/10.3390/polym12030608.
[20] S. Ventura-Cruz, A. Tecante, Extraction and characterization of cellulose nanofibers from Rose stems (Rosa spp.), Carbohydr. Polym. 220 (2019) 53–59.
[21] E. Pinto, W.N. Aggrey, P. Boakye, G. Amenuvor, Y.A. Sokama-Neuyam, M. K. Fokuo, H. Karimaie, K. Sarkodie, C.D. Adenutsi, S. Erzuah, M.A.D. Rockson, Cellulose processing from biomass and its derivatization into carboxymethylcellulose: a review, S. African 15 (2022) e01078, https://doi.org/10.1016/j.sciaf.2021.e01078.
[22] S. Horikoshi, R.F. Schiffmann, J. Fukushima, N. Serpone, Microwave chemical and materials processing, in: Microwave Chemical and Materials Processing, Springer, Singapore; Singapore, 2018, pp. 33–45.

[23] M. Broda, D.J. Yelle, K. Serwańska, Bioethanol production from lignocellulosic biomass—challenges and solutions, Molecules 27 (2022) 8717, https://doi.org/10.3390/molecules27248717.
[24] N. Sweygers, J. Harrer, R. Dewil, L. Appels, A microwave-assisted process for the in-situ production of 5-hydroxymethylfurfural and furfural from lignocellulosic polysaccharides in a biphasic reaction system, J. Clean. Prod. 187 (2018) 1014–1024, https://doi.org/10.1016/j.jclepro.2018.03.204.
[25] Z. Zhao, H. Li, X. Gao, Microwave encounters ionic liquid: synergistic mechanism, synthesis and emerging applications, Chem. Rev. (2023).
[26] I.N. Sudiana, S. Mitsudo, T. Nishiwaki, P.E. Susilowati, L. Lestari, M.Z. Firihu, H. Aripin, Synthesis and characterization of microwave sintered silica xerogel produced from rice husk ash, J. Phys. Conf. Ser. 739 (2016) 012059, https://doi.org/10.1088/1742-6596/739/1/012059.
[27] X. Liu, Z. Qin, Y. Ma, H. Liu, X. Wang, Cellulose-based films for food packaging applications: review of preparation, properties, and prospects, J. Renew. Mater. 11 (2023) 3203–3225, https://doi.org/10.32604/jrm.2023.027613.
[28] A.K. Babu, G. Kumaresan, V.A.A. Raj, R. Velraj, Review of leaf drying: mechanism and influencing parameters, drying methods, nutrient preservation, and mathematical models, Renew. Sustain. Energy Rev. 90 (2018) 536–556, https://doi.org/10.1016/j.rser.2018.04.002.
[29] M. Mahendradatta Khaerunnisa, M. Asfar, Characteristics of simplicia ginger (Zingiber officinale) and lemongrass (Cymbopogon citratus) powder by different drying method, IOP Conf. Ser. Earth Environ. Sci. 807 (2021) 022052, https://doi.org/10.1088/1755-1315/807/2/022052.
[30] S. Yadav, S. Mishra, Moisture sorption isotherms and storage study of spray-dried probiotic finger millet milk powder, J. Stored Prod. Res. 102 (2023) 102128, https://doi.org/10.1016/j.jspr.2023.102128.
[31] M. Li, Y.-L. Cheng, N. Fu, D. Li, B. Adhikari, X.D. Chen, Isolation and characterization of corncob cellulose fibers using microwave-assisted chemical treatments, Int. J. Food Eng. 10 (2014) 427–436, https://doi.org/10.1515/ijfe-2014-0052.
[32] S.T.C.L. Ndruru, D. Wahyuningrum, B. Bundjali, I.M. Arcana, Green simple microwave-assisted extraction (MAE) of cellulose from Theobroma cacao L.(TCL) husk, in: IOP Conference Series: Materials Science and Engineering, IOP Publishing, 2019.
[33] A. Martinsson, M. Hasani, A. Potthast, H. Theliander, Modification of softwood kraft pulp fibres using hydrogen peroxide at acidic conditions, Cellulose 27 (2020) 7191–7202, https://doi.org/10.1007/s10570-020-03245-z.
[34] S. Agarwal, M. Hoque, N. Bandara, K. Pal, P. Sarkar, Synthesis and characterization of tamarind kernel powder-based antimicrobial edible films loaded with geraniol, Food Packag. Shelf Life 26 (2020) 100562, https://doi.org/10.1016/j.fpsl.2020.100562.
[35] G. Xu, M. Li, P. Lu, Experimental investigation on flow properties of different biomass and torrefied biomass powders, Biomass Bioenergy 122 (2019) 63–75, https://doi.org/10.1016/j.biombioe.2019.01.016.
[36] M. Rizwan, S.R. Gilani, A.I. Durrani, S. Naseem, Low temperature green extraction of Acer platanoides cellulose using nitrogen protected microwave assisted extraction (NPMAE) technique, Carbohydr. Polym. (2021).
[37] H.S. Hafid, F.N. Omar, J. Zhu, M. Wakisaka, Enhanced crystallinity and thermal properties of cellulose from rice husk using acid hydrolysis treatment, Carbohydr. Polym. 260 (2021) 117789, https://doi.org/10.1016/j.carbpol.2021.117789.
[38] J. Gichuki, P.G. Kareru, A.N. Gachanja, C. Ngamau, Characteristics of microcrystalline cellulose from coir fibers, J. Nat. Fibers 19 (2022) 915–930, https://doi.org/10.1080/15440478.2020.1764441.
[39] W. Klunklin, K. Jantanasakulwong, Y. Phimolsiripol, N. Leksawasdi, P. Seesuriyachan, T. Chaiyaso, C. Insomphun, S. Phongthai, P. Jantrawut, S. R. Sommano, W. Punyodom, A. Reungsang, T.M.P. Ngo, P. Rachtanapun, Synthesis, characterization, and application of carboxymethyl cellulose from Asparagus stalk end, Polymers 13 (2020) 81, https://doi.org/10.3390/polym13010081.
[40] A.C.F. Louis, S. Venkatachalam, Energy efficient process for valorization of corn cob as a source for nanocrystalline cellulose and hemicellulose production, Int. J. Biol. Macromol. 163 (2020) 260–269, https://doi.org/10.1016/j.ijbiomac.2020.06.276.
[41] G. Zhang, L. Zhang, H. Deng, P. Sun, Preparation and characterization of sodium carboxymethyl cellulose from cotton stalk using microwave heating, J. Chem. Technol. Biotechnol. 86 (2011) 584–589, https://doi.org/10.1002/jctb.2556.
[42] n.d.). https://www.cell.com/heliyon/pdf/S2405-8440(22)00402-9.pdf (accessed February 28, 2024).
[43] B. Ahmed, J. Gwon, M. Thapaliya, A. Adhikari, S. Ren, Q. Wu, Combined effects of deep eutectic solvent and microwave energy treatments on cellulose fiber extraction from hemp bast, Cellulose 30 (2023) 2895–2911, https://doi.org/10.1007/s10570-023-05081-3.
[44] Q. Wang, S. Xiao, S.Q. Shi, L. Cai, Microwave-assisted formic acid extraction for high-purity cellulose production, Cellulose 26 (2019) 5913–5924, https://doi.org/10.1007/s10570-019-02516-8.
[45] Y. Liu, B. Sun, X. Zheng, L. Yu, J. Li, Integrated microwave and alkaline treatment for the separation between hemicelluloses and cellulose from cellulosic fibers, Bioresour. Technol. 247 (2018) 859–863, https://doi.org/10.1016/j.biortech.2017.08.059.
[46] J.I. Duruaku, P.A. Okoye, N.H. Okoye, J.O. Nwadiogbu, V.I. Onwukeme, R. U. Arinze, An evaluation of the physicochemical, structural and morphological properties of selected tropical wood species for possible utilization in the wood industry, J. Sustain. Bioenergy Syst. 13 (2023) 131–148.
[47] https://ir.unilag.edu.ng/handle/123456789/7815 (accessed February 28, 2024).
[48] A.A. Sundarraj, T.V. Ranganathan, Extraction and functional properties of cellulose from jackfruit (Artocarpus integer) Waste, Int. J. Pharma Sci. Res. 9 (2018) 1000–1008.
[49] D.M. Parid, N.A. Abd Rahman, A.S. Baharuddin, M.A.P. Mohammed, A.M. Johari, S.Z.A. Razak, Synthesis and characterization of carboxymethyl cellulose from oil palm empty fruit bunch stalk fibres, Bioresources 13 (2018) 535–554.
[50] ñhttps://d1wqtxts1xzle7.cloudfront.net/63752161/Deepa_520200626-103800-1jeu09d-libre.pdf?1593222559=&response-content-disposition=inline;+filename=Optimizing_alkali_concentration_and_stee.pdf&Expires=1709138055&Signature=TZuAsrtsYpHu2I8Hv1GFTE5xENBWyHuNv4eCBjH8hC7msnkd6PCDomIU9U3I~Z~QOSxbEkdvddcK188JE2hnGpSAItiyHQWW6GnYOs6IRyuwCptfhuuFOncBdTtNyI79uBHSIfHayVvF0vtEd9hWoe9zyZgswaFix4iJ7-ozJQUThs0YghmanseruxNKUt5ñqXFfoKBulZGukSPNHFZuK513uWY0cQd~8yTC~ncXDK8VXYVK0v0hhrdCrwzf4UQyLdsYbE9atSVX20mPPNo0ZgvMUsiai-m4LDFfZpYLqHO2KDnN09I~q9Xlh3ovz2SHGew34TE-iJtjqaHCvpgyQ__&Key-Pair-Id=APKAJLOHF5GGSLRBV4ZA (accessed February 28, 2024).
[51] S. Tasnim, M.F.K. Tipu, M.S. Rana, M.A. Rahim, M. Haque, M.S. Amran, A. A. Chowdhury, J.A. Chowdhury, Modification of bulk density, flow property and crystallinity of microcrystalline cellulose prepared from waste cotton, Materials 16 (2023), https://doi.org/10.3390/ma16165664.
[52] E.V. Ndika, U.S. Chidozie, U.K. Ikechukwu, Chemical modification of cellulose from palm kernel de-oiled cake to microcrystalline cellulose and its evaluation as a pharmaceutical excipient, Afr. J. Pure Appl. Chem. 13 (2019) 49–57.
[53] n.d.). https://aaltodoc.aalto.fi/items/db2ec4ee-3aef-46cb-9613-ac4bf9cb3651 (accessed February 28, 2024).
[54] B. Lindman, G. Karlström, L. Stigsson, On the mechanism of dissolution of cellulose, J. Mol. Liq. 156 (2010) 76–81, https://doi.org/10.1016/j.molliq.2010.04.016.
[55] B. Medronho, A. Romano, M.G. Miguel, L. Stigsson, B. Lindman, Rationalizing cellulose (in)solubility: reviewing basic physicochemical aspects and role of hydrophobic interactions, Cellulose 19 (2012) 581–587, https://doi.org/10.1007/s10570-011-9644-6.
[56] T. Budtova, P. Navard, Cellulose in NaOH–water based solvents: a review, Cellulose 23 (2016) 5–55, https://doi.org/10.1007/s10570-015-0779-8.
[57] M. Kihlman, F. Aldaeus, F. Chedid, U. Germgård, Effect of various pulp properties on the solubility of cellulose in sodium hydroxide solutions, Holzforschung 66 (2012) 601–606, https://doi.org/10.1515/hf-2011-0220.
[58] B. Swensson, A. Larsson, M. Hasani, Probing interactions in combined hydroxide base solvents for improving dissolution of cellulose, Polymers 12 (2020) 1310, https://doi.org/10.3390/polym12061310.
[59] B. Medronho, B. Lindman, Competing forces during cellulose dissolution: from solvents to mechanisms, Curr. Opin. Colloid Interface Sci. 19 (2014) 32–40, https://doi.org/10.1016/j.cocis.2013.12.001.
[60] B. Lindman, B. Medronho, G. Karlström, Clouding of nonionic surfactants, Curr. Opin. Colloid Interface Sci. 22 (2016) 23–29, https://doi.org/10.1016/j.cocis.2016.01.005.
[61] P. Bardhan, K.S.H. Eldiehy, N. Daimary, M. Gohain, V.V. Goud, D. Deka, M. Mandal, Structural characterization of mixed rice straw and deoiled algal cake-based substrate as a potential bioenergy feedstock for microbial lipids and carotenoid production, Waste Biomass Valorization 13 (2022) 195–212, https://doi.org/10.1007/s12649-021-01512-z.
[62] B. Liu, W. Li, Y. Xu, H. Zhang, R. Cai, Z. Guo, L. Zhou, J. Zhang, Y. Yuan, Mechanism of cellulose regeneration from its ionic liquid solution as revealed by infrared spectroscopy, Polymer 257 (2022) 125280, https://doi.org/10.1016/j.polymer.2022.125280.
[63] R. Hernandez Perez, A. Olarte Paredes, R. Salgado Delgado, A.M. Salgado Delgado, Rice husk Var.'Morelos A-2010'as an eco-friendly alternative for the waste management converting them cellulose and nanocellulose, Int. J. Environ. Anal. Chem. 103 (2023) 7571–7586.
[64] K.S. Salem, N.K. Kasera, M.A. Rahman, H. Jameel, Y. Habibi, S.J. Eichhorn, A. D. French, L. Pal, L.A. Lucia, Comparison and assessment of methods for cellulose crystallinity determination, Chem. Soc. Rev. 52 (2023) 6417–6446, https://doi.org/10.1039/d2cs00569g.
[65] L. Klaai, D. Hammiche, A. Boukerrou, V. Pandit, Thermal and structural analyses of extracted cellulose from olive husk, Mater. Today 52 (2022) 104–107, https://doi.org/10.1016/j.matpr.2021.10.498.
[66] A.D. French, M. Santiago Cintrón, Cellulose polymorphy, crystallite size, and the segal crystallinity index, Cellulose 20 (2013) 583–588, https://doi.org/10.1007/s10570-012-9833-y.
[67] A.F. Sahayaraj, M.T. Selvan, I. Jenish, M. Ramesh, Extraction and characterization of novel cellulosic fiber from Jatropha integerrima plant stem for potential reinforcement in polymer composites, Biomass Convers. Biorefin. (2023), https://doi.org/10.1007/s13399-023-04541-x.
[68] G. Kłosowski, D. Mikulski, Changes in various lignocellulose biomasses structure after microwave-assisted hydrotropic pretreatment, Renew. Energy (2023).
[69] O. Zabihi, M. Ahmadi, C. Liu, R. Mahmoodi, Q. Li, M. Naebe, Development of a low cost and green microwave assisted approach towards the circular carbon fibre composites, Compos. B Eng. 184 (2020) 107750, https://doi.org/10.1016/j.compositesb.2020.107750.
[70] Q. Lin, Y. Huang, W. Yu, Effects of extraction methods on morphology, structure and properties of bamboo cellulose, Ind. Crops Prod. 169 (2021) 113640, https://doi.org/10.1016/j.indcrop.2021.113640.
[71] U. Qasim, Z. Ali, M.S. Nazir, S. Ul Hassan, S. Rafiq, F. Jamil, A.H. Al-Muhtaseb, M. Ali, M.B. Khan Niazi, N.M. Ahmad, S. Ullah, A. Mukhtar, S. Saqib, Isolation of

cellulose from wheat straw using alkaline hydrogen peroxide and acidified sodium chlorite treatments: comparison of yield and properties, Adv. Polym. Technol. 2020 (2020) 1–7, https://doi.org/10.1155/2020/9765950.

[72] N.A. Abdullah, M.H. Sainorudin, M.S.A. Rani, M. Mohammad, N.H. Abd Kadir, N. Asim, Structure and thermal properties of microcrystalline cellulose extracted from coconut husk fiber, Polimery 66 (2021) 187–192.

[73] V. Jeyabalaji, G.R. Kannan, P. Ganeshan, K. Raja, B. Nagarajaganesh, P. Raju, Extraction and characterization studies of cellulose derived from the roots of Acalypha indica L, J. Nat. Fibers 19 (2022) 4544–4556.

[74] n.d.). https://www.cell.com/heliyon/pdf/S2405-8440(21)00783-0.pdf (accessed February 28, 2024).

[75] S.B.B.P.J. Sahu, S. Nayak, S. Sahu, J. Mohapatra, S.K. Khuntia, P.K. Sahoo, B. B. Nayak, Extraction and characterization of natural cascabela Thevetia bast fibers: a potential candidate as reinforcement in epoxy composites, J. Nat. Fibers 20 (2023).